Supplement of Geosci. Model Dev., 18, 3799–3817, 2025
https://doi.org/10.5194/gmd-18-3799-2025-supplement

Geoscientific Model Development
Open Access

Supplement of

Process-based modeling framework for sustainable irrigation management at the regional scale: integrating rice production, water use, and greenhouse gas emissions

Yan Bo et al.

Correspondence to: Feng Zhou (zhouf@pku.edu.cn)

Supplementary Tables

Table S1 Summary table of model input data.

Table S2 Effect of non-continuous flooding irrigation on leaf area index (R^{LAI}) under different levels of the lowest threshold of soil water potential (SWP) at different relative growth stages (RDS).

Table S3 Effect of non-continuous flooding irrigation on net photosynthetic rate (R^{Pn}) under different levels of the lowest threshold of soil water potential (SWP) at different relative growth stages (RDS).

Table S4 Effect of non-continuous flooding irrigation on harvest index (R^{HI}) under different levels of the lowest threshold of soil water potential.

Table S5 Scenario designs of the simulation experiments to isolate contribution of each physiological functions to ΔYield.

Table S6 Genetic parameters for 51 rice cultivars.

Supplementary Figures

Figure S1 Observation dataset of water management effects and its representativeness.

Figure S2 Effects of non-continuous flooding on (a) leaf area index, (b) net photosynthetic rate and (c) harvest index based on experimental observations.

Figure S3 Model performance in simulating spatial pattern of (a) rice yield, (b) irrigation water use, (c) methane and (d) nitrous oxide emissions under continuous flooding (baseline).

Figure S4 Spatial pattern of model parameters under continuous flooding for the major and second rice growing season.

Figure S5 Parameter transfer functions for upscaling model parameters.

Figure S6 Model performance in simulating rice yield (a-b) and irrigation water use (b and d) based on the origin (a, c) and modified (b, d) WHCNS model.

Figure S7 Model performance in simulating cultivar differences in ΔYield before (a) and after (b) model modification.

Figure S8 Contribution of physiological processes to ΔYield and relationship with predictors.

Figure S9 Scenario simulations and comparison with observations.

Figure S10 Distribution of dominant drivers regulating variation in relative changes of (a) Yield, (b) IRR, (c) CH_4, (d) N_2O.

Figure S11 The same as Fig. S9 but for 2.5°-by-2.5° moving windows.

Figure S12 Spatial pattern of NCF benefits under four optimization targets based on the origin and modified model.

Figure S13 Spatial pattern of lower irrigation threshold under four optimization targets based on the origin and modified model.

Figure S14 Tradeoffs between regulation potentials of different target variables.

Table S1 Summary table of model input data.

Category	Variables	Spatial resolution and sources
Climate (daily)	Mean air temperature, °C Maximum air temperature, °C Minimum air temperature, °C Wind speed, m s^{-1} Precipitation, mm Humidity, % Downward solar radiation, W m^{-2}	0.25 × 0.25° the fifth generation ECMWF reanalysis (ERA5) (Hersbach et al., 2018)
Soil (5, 15, 30, 60, 100, 200 cm depth)	Bulk density, g cm^{-3} Clay contents, % Saturated water content, cm^3 cm^{-3} Field water capacity, cm^3 cm^{-3} Wilting point, cm^3 cm^{-3} Saturated hydraulic conductivity, cm day^{-1}	10 × 10 km SoilGrids (Han et al., 2015)
Management	Planting date, year/month/day Harvest date, year/month/day	0.5 × 0.5° GGCMI Phase 3 (Jägermeyr et al., 2021)
	Fertilizer rate, kg N ha^{-1} Fertilizer timing, year/month/day	0.5 × 0.5° Simulated by the auto-fertilization component
	Upper irrigation threshold, mm Lower irrigation threshold, mm or kpa Maximum allowable field water level after rainfall, mm	Station Table A1 Chen et al. (2022)

References

Hersbach, H., Bell, B., Berrisford, P., Biavati, G., Horányi, A., Muñoz Sabater, J., Nicolas, J., Peubey, C., Radu, R., Rozum, I., Schepers, D., Simmons, A., Soci, C., Dee, D., Thépaut, J.-N.: ERA5 hourly data on single levels from 1979 to present. Copernicus Climate Change Service (C3S) Climate Data Store (CDS). (Accessed on < 06-10-2021>), 10.24381/cds.adbb2d47, 2018.

Han, E. I., Amor; Koo, Jawoo "Global High-Resolution Soil Profile Database for Crop Modeling Applications", http://dx.doi.org/10.7910/DVN/1PEEY0, Harvard Dataverse, V1, 2015.

Jägermeyr, J., Müller, C., Ruane, A. C., Elliott, J., Balkovic, J., Castillo, O., Faye, B., Foster, I., Folberth, C., Franke, J. A., Fuchs, K., Guarin, J. R., Heinke, J., Hoogenboom, G., Iizumi, T., Jain, A. K., Kelly, D., Khabarov, N., Lange, S., Lin, T.-S., Liu, W., Mialyk, O., Minoli, S., Moyer, E. J., Okada, M., Phillips, M., Porter, C., Rabin, S. S., Scheer, C., Schneider, J. M., Schyns, J. F.,

Skalsky, R., Smerald, A., Stella, T., Stephens, H., Webber, H., Zabel, F., and Rosenzweig, C.: Climate impacts on global agriculture emerge earlier in new generation of climate and crop models, Nature Food, 2, 873-885, 10.1038/s43016-021-00400-y, 2021.
Chen, M., Linker, R., Wu, C., Xie, H., Cui, Y., Luo, Y., Lv, X., and Zheng, S.: Multi-objective optimization of rice irrigation modes using ACOP-Rice model and historical meteorological data, Agr Water Manage, 272, 107823, https://doi.org/10.1016/j.agwat.2022.107823, 2022.

Table S2 Effect of non-continuous flooding irrigation on leaf area index (R^{LAI}) under different levels of the lowest threshold of soil water potential (SWP) at different relative growth stages (RDS). The effect values in the table was mean values of observations under correspond SWP and RDS levels (see figure S1a). Effects under other SWP and RDS levels was determined by bilinear interpolation.

RDS	Soil water potential (kpa)										
	-100	**-60**	**-50**	**-40**	**-30**	**-25**	**-20**	**-15**	**-10**	**-5**	**0**
0 (Planting)	0.000	1.000	1.000	1.000	1.000	1.000	1.000	1.000	1.000	1.000	1.000
0.20 (Tillering)	0.000	0.976	0.976	0.976	0.976	0.976	0.976	0.976	0.976	0.976	1.000
0.40 (Booting)	0.000	0.563	0.667	0.745	0.836	0.869	0.902	0.963	0.961	1.138	1.000
0.55 (Heading)	0.000	0.689	0.799	0.879	0.890	1.015	0.955	1.018	0.986	1.028	1.000
1 (Maturity)	0.000	0.529	0.621	0.792	0.859	0.910	0.962	1.275	1.282	1.191	1.000

Table S3 Effect of non-continuous flooding irrigation on net photosynthetic rate (R^{Pn}) under different levels of the lowest threshold of soil water potential (SWP) at different relative growth stages (RDS). The effect values in the table was mean values of observations under correspond SWP and RDS levels (see figure S1b). Effects under other SWP and RDS levels was determined by bilinear interpolation.

RDS	**Soil water potential (kpa)**						
	-100	**-30**	**-20**	**-15**	**-10**	**-5**	**0**
0 (Planting)	1.000	1.000	1.000	1.000	1.000	1.000	1.000
0.20(Tillering)	1.000	1.000	1.038	1.214	1.224	1.175	1.000
0.75(Grain filling)	1.000	1.069	1.144	1.318	1.356	1.300	1.000
1 (Maturity)	1.000	1.000	1.000	1.000	1.000	1.000	1.000

Table S4 Effect of non-continuous flooding irrigation on harvest index (R^{HI}) under different levels of the lowest threshold of soil water potential. Effects under other SWP levels was determined by linear interpolation. The effect values in the table was mean values of observations under correspond SWP level (see figure S1c). Effects under other SWP levels was determined by linear interpolation.

Soil water potential (kpa)	-1500	-60	-50	-40	-30	0
Factor	0.755	0.755	0.872	0.939	1.025	1.000

Table S5 Scenario designs of the simulation experiments to isolate contribution of each physiological functions to ΔYield.

Scenario	f_{LAI}	f_{Pn}	f_{HI}	Contribution
S1	Yes	Yes	Yes	/
S2	No	Yes	Yes	$\Delta Yield^{LAI}$=ΔYield (S1)- ΔYield (S2)
S3	Yes	No	Yes	$\Delta Yield^{Pn}$=ΔYield (S1)- ΔYield (S3)
S4	Yes	Yes	No	$\Delta Yield^{HI}$=ΔYield (S1)- ΔYield (S4)

Table S6 Genetic parameters for 51 rice cultivars.

Cultivar name	*Cumtemp*	*AMIN*	P^{LAI}	P^{Pn}	P^{HI}
Annada	1816.9	0.20	4.04	0.66	5.31
Apo	1816.9	0.20	2.92	0.75	1.12
BRRIDhan28	1280.6	0.32	0.00	0.00	0.08
Changyou5	1949.3	0.36	0.00	0.45	0.00
Dexiang4103	1819.4	0.32	1.44	3.46	4.02
DN425	1265.1	0.30	1.88	0.00	0.16
Gaoshan1	1580.2	0.37	1.02	1.01	1.01
GB1	1820.7	0.24	2.94	0.00	0.34
HD5	1886.5	0.29	1.25	3.00	1.47
HHZ	1481.3	0.41	1.21	1.34	1.17
HY113	1777.3	0.33	0.00	1.64	1.63
HY3	2013.1	0.26	1.41	1.30	0.01
HY8	1871.7	0.34	0.00	0.05	0.00
IET4786	1413.9	0.33	2.43	0.01	0.43
IR36	1700.4	0.24	2.27	0.01	0.72
IR71706	1393.5	0.28	0.10	0.00	0.28
IR72	1669.9	0.28	0.84	0.00	4.49
Jinkeyou938	1957.9	0.30	2.72	0.35	0.00
Koshihikari	1771.9	0.23	14.51	0.35	0.36
Liangyoupeijiu	1909.9	0.34	7.73	0.00	0.00
Lianjing7	2046.7	0.27	0.18	3.45	1.89
Lingxiangyou18	1871.7	0.31	2.46	0.09	0.00
Lvhan1	1580.2	0.33	4.92	5.08	10.00
Naveen	1816.9	0.23	4.81	0.01	5.84
Nei5You8015	1378.4	0.58	0.00	0.01	0.06
Nipponbare	1469.1	0.30	1.63	0.04	0.01
PAU201	1879.2	0.30	2.18	0.44	0.58
PR113	1604.5	0.30	1.40	0.50	0.88
PSBRc80	1773.4	0.29	0.04	0.01	0.01
Pusa1509	2456.9	0.19	0.00	0.01	0.01
Satabdi	1816.9	0.21	5.64	2.95	3.20
Sensho	1836.2	0.22	0.00	0.00	0.03
Shendao529	1557.7	0.27	0.01	4.26	8.97
Shennong9765	1426.3	0.28	2.54	0.15	0.01
SS6	1265.1	0.38	2.00	0.11	0.64
Tainan11	2450.2	0.14	0.00	0.05	0.10
Tainong84	1999.7	0.21	10.00	0.01	0.00
Tianyouhuazhan	1777.3	0.37	0.00	0.18	0.00
TY3618	1468.0	0.43	1.99	1.00	1.02
UPLRi7	1913.8	0.22	6.12	2.57	0.16

WFY	1113.8	0.54	0.00	0.00	0.06
WYJ24	1814.1	0.36	0.01	0.08	0.01
YangDao6	1933.1	0.30	0.84	1.15	1.08
YangJing4038	1909.9	0.30	0.22	1.65	1.33
Yixiang3724	1819.4	0.29	0.43	3.20	3.43
YLY	1664.7	0.36	5.36	0.00	0.31
YY2640	1886.5	0.33	2.26	3.96	2.65
YY4949	1969.9	0.25	2.12	0.95	0.84
ZJZ17	979.4	0.45	0.02	0.11	0.04
ZZY	2096.2	0.32	0.58	0.94	0.96
PR118	2863.8	0.18	10.00	0.03	0.01

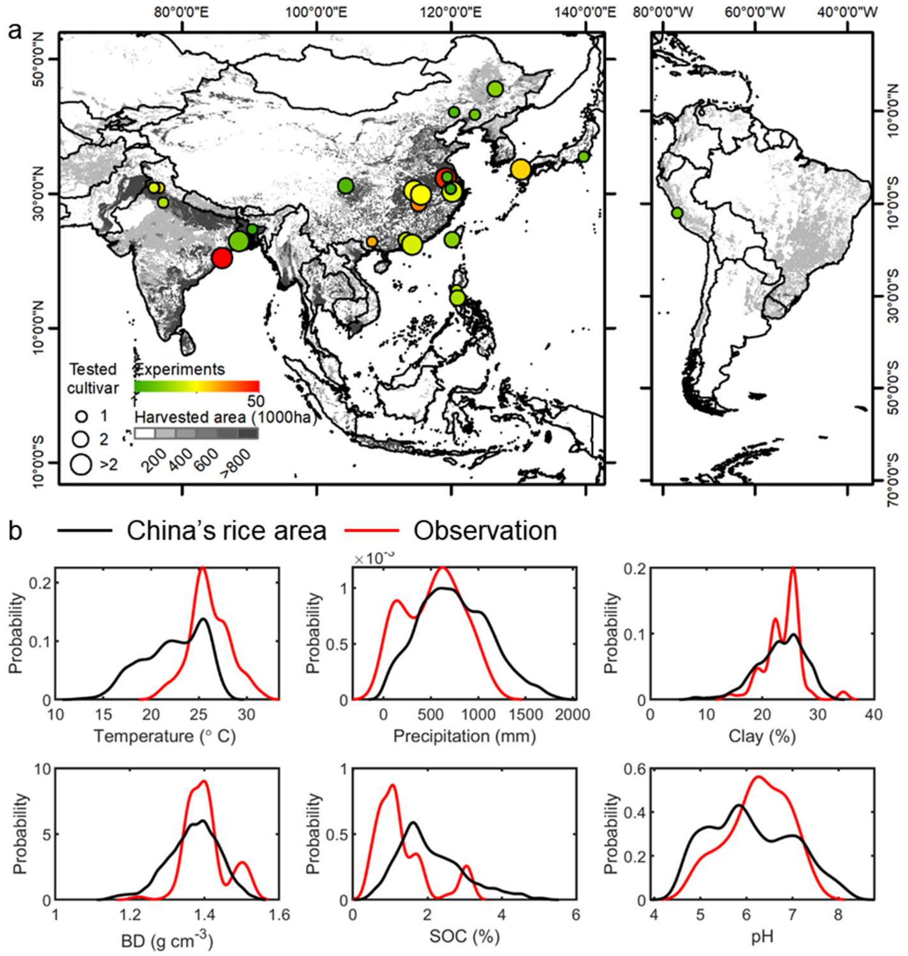

Figure S1 Observation dataset of water management effects and its representativeness. (a) Spatial distribution of observation sites. Dot color indicates the number of experiments, and dot size indicates the number of tested cultivars. The gray area represents irrigated rice areas. **(b)** Comparison of probability density of climate and soil factors between our observation dataset (red) and China's rice areas (black).

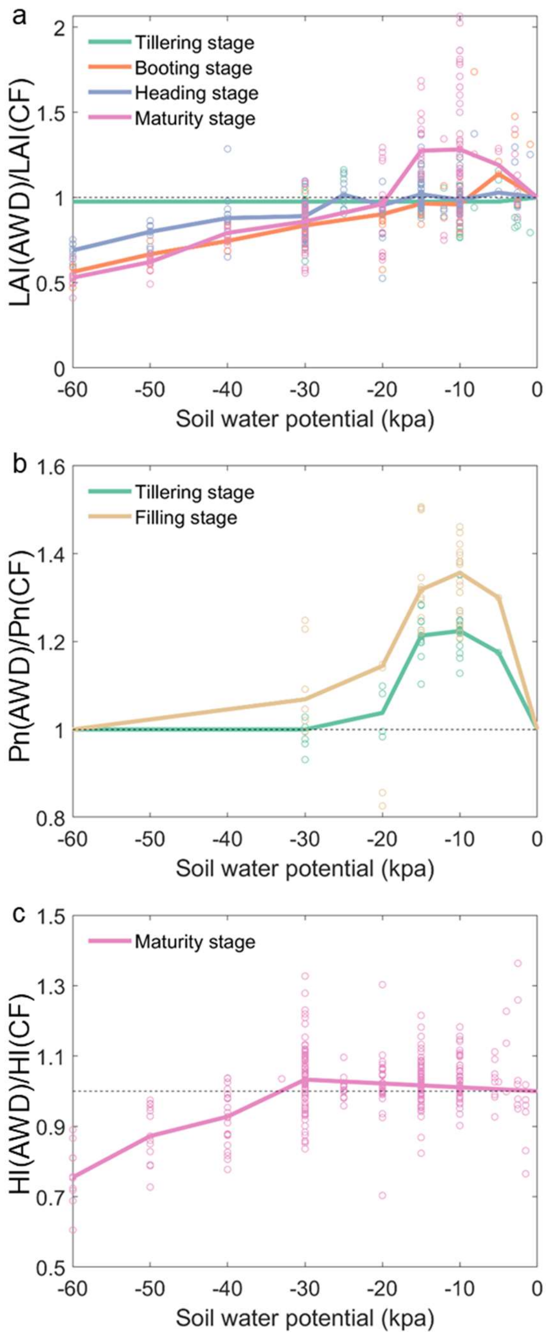

Figure S2 Effects of non-continuous flooding on (a) leaf area index, (b) net photosynthetic rate and (c) harvest index based on experimental observations. The dots represent ratio of physiological traits under treatment to that under control. The solid lines were derived by linear interpolation of mean observations. *LAI*, *Pn* and *HI* represent leaf area index, net photosynthetic rate and harvest index, respectively. Different color in the same subplot represent effects of different growth stages.

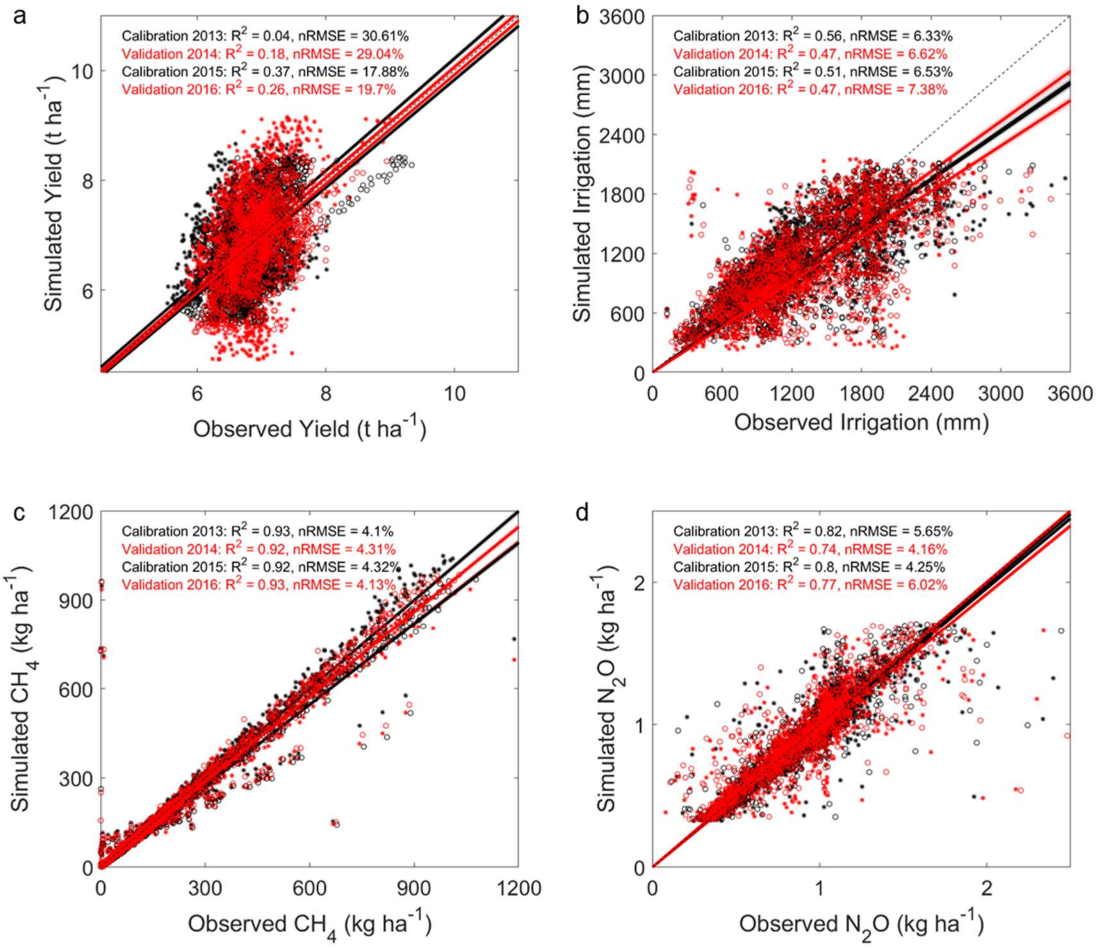

Figure S3 Model performance in simulating spatial pattern of (a) rice yield, (b) irrigation water use, (c) methane and (d) nitrous oxide emissions under continuous flooding (baseline). Black and red dots respectively show performance of calibration (2013 and 2015) and validation periods (2014 and 2016). The lines are the linear regression lines with shaded areas around representing the 95% confidence interval.

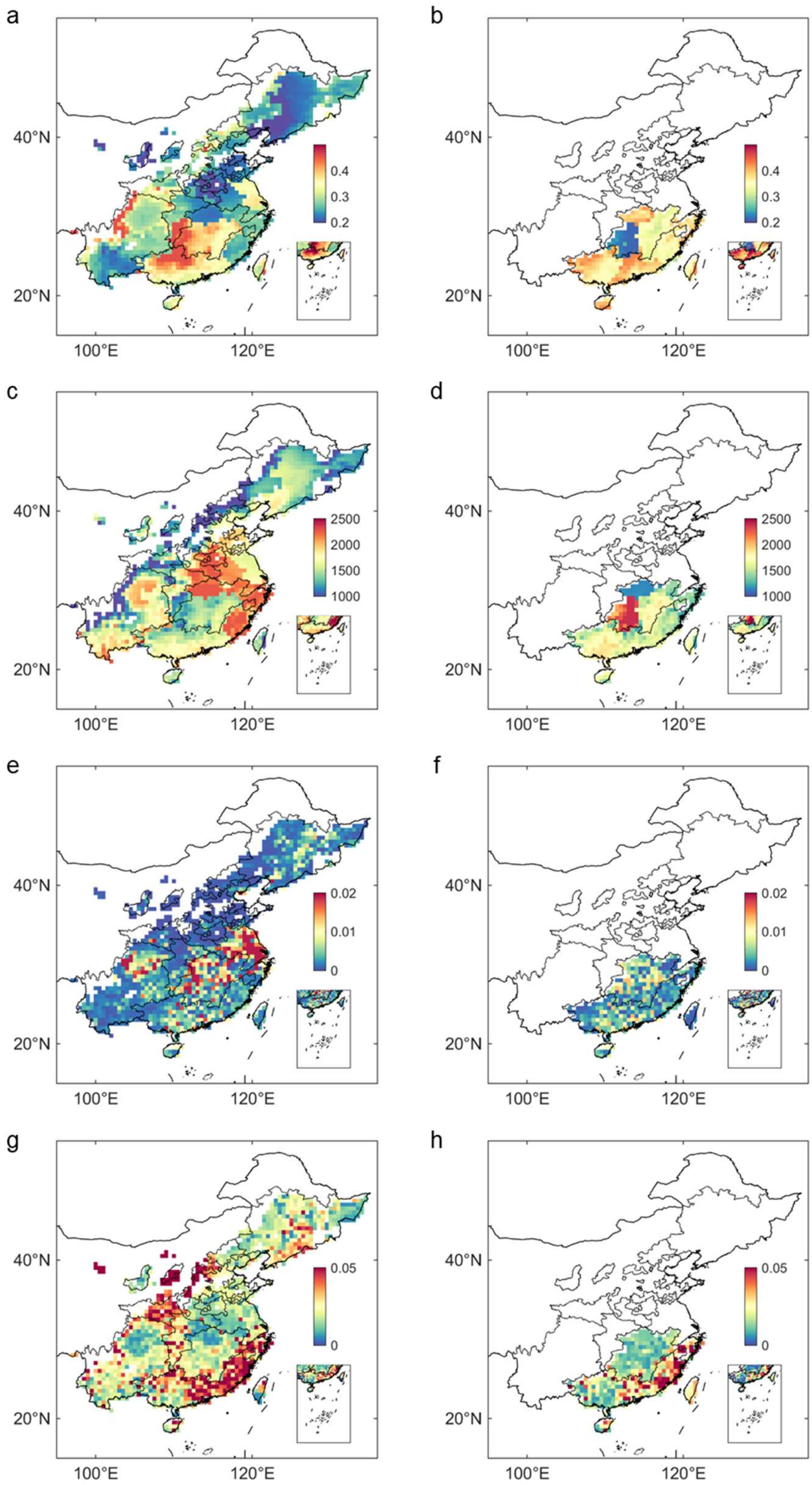

Figure S4 Spatial pattern of model parameters under continuous flooding for the major and second rice growing season. **(a-b)** minimum assimilation rates per day (*AMIN*). **(c-d)** Effective cumulative temperature for rice maturity (*Cumtemp*, °C). **(e-f)** maximum CH_4 production rate per soil weight at 30 °C (*MPmax,* g C g^{-1} d^{-1}). **(g-h)** maximum portion of denitrification to N_2O production (f_{N2O_d}).

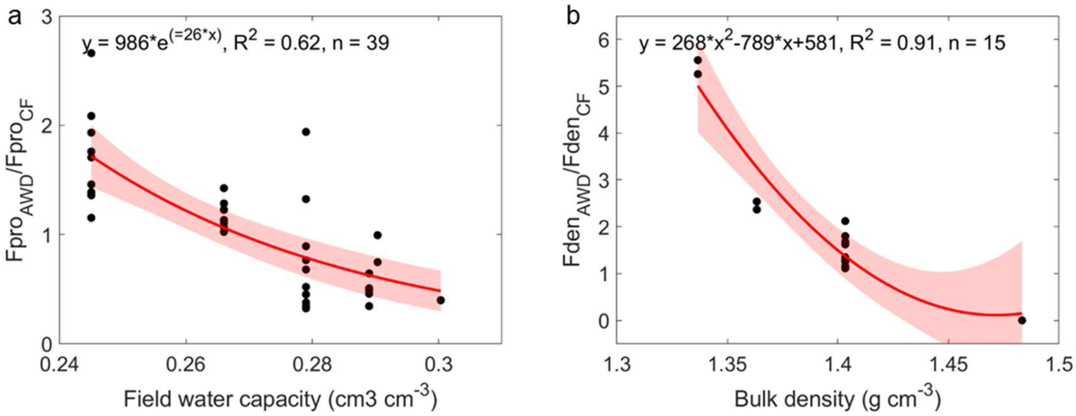

Figure S5 Parameter transfer functions for upscaling model parameters. (a) Relationship between field water capacity and ratio of the maximum CH_4 production rate per soil weight at 30 °C (*MPmax*) under AWD to CF. **(b)**Relationship between field water capacity and ratio of maximum portion of denitrification to N2O production (f_{N2O_d}) under AWD to CF.

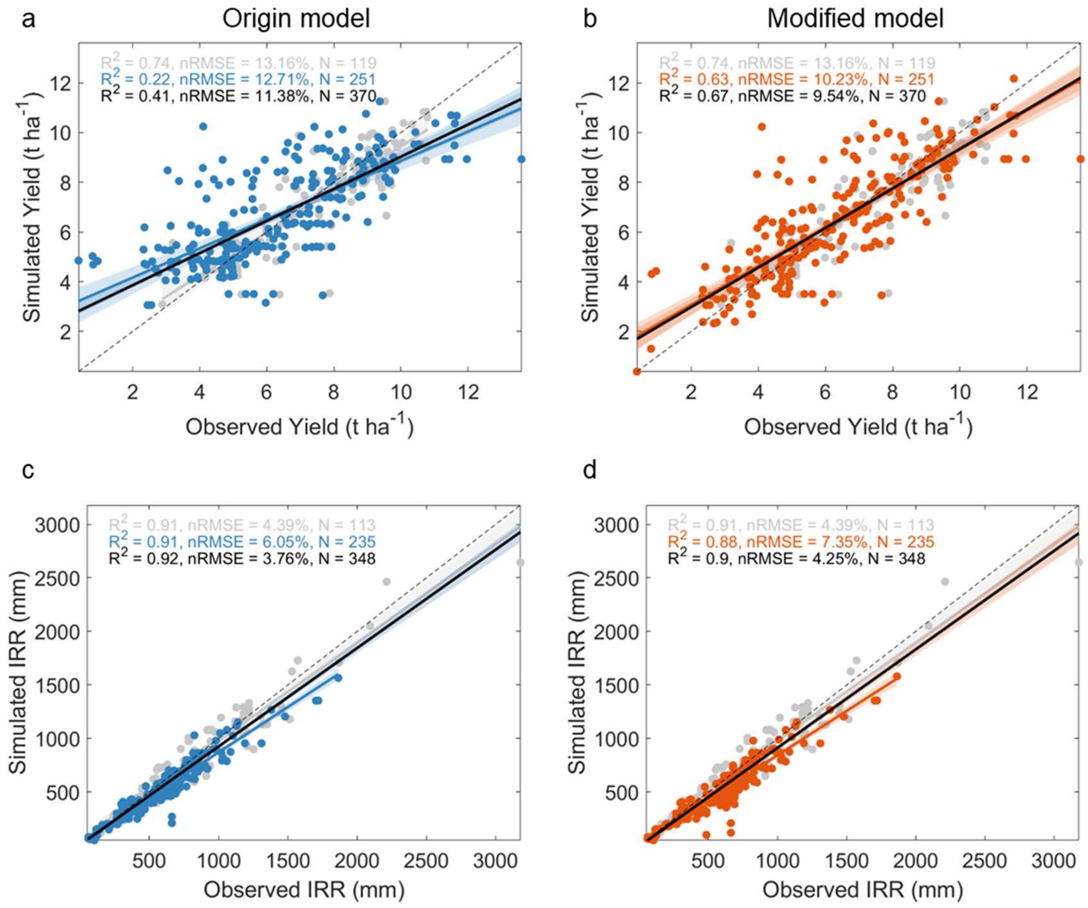

Figure S6 Model performance in simulating rice yield (a-b) and irrigation water use (b and d) based on the origin (a, c) and modified (b, d) WHCNS model. The solid lines are the linear regression lines with the shaded areas around each line representing the 95% confidence interval. The dashed lines are 1:1 lines. The gray color indicates results under continuous flooding conditions (CF, control). The blue and orange color indicate results under non-continuous flooding conditions (NCF, treatment) based on the origin model and modified model, respectively. The dark lines are regression lines for all records of CF and NCF conditions.

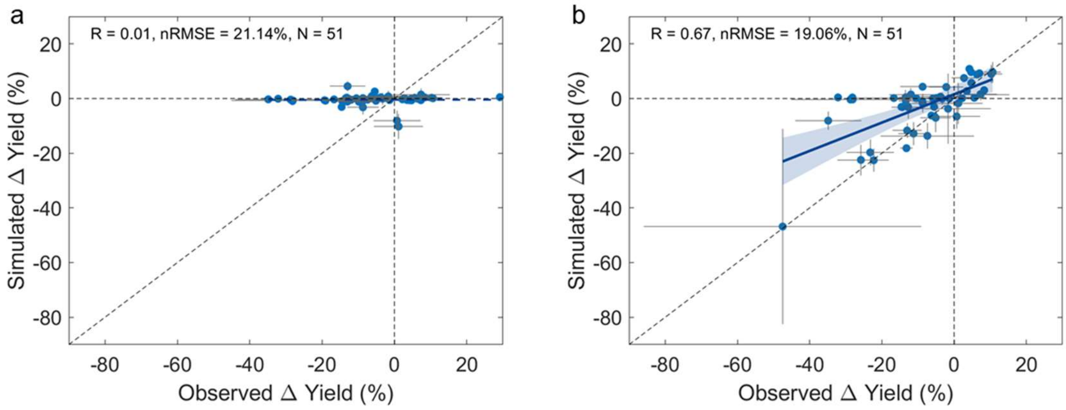

Figure S7 Model performance in simulating cultivar differences in ΔYield before (a) and after (b) model modification. The dot and error bar indicate mean and standard error of ΔYield for 51 rice cultivars.

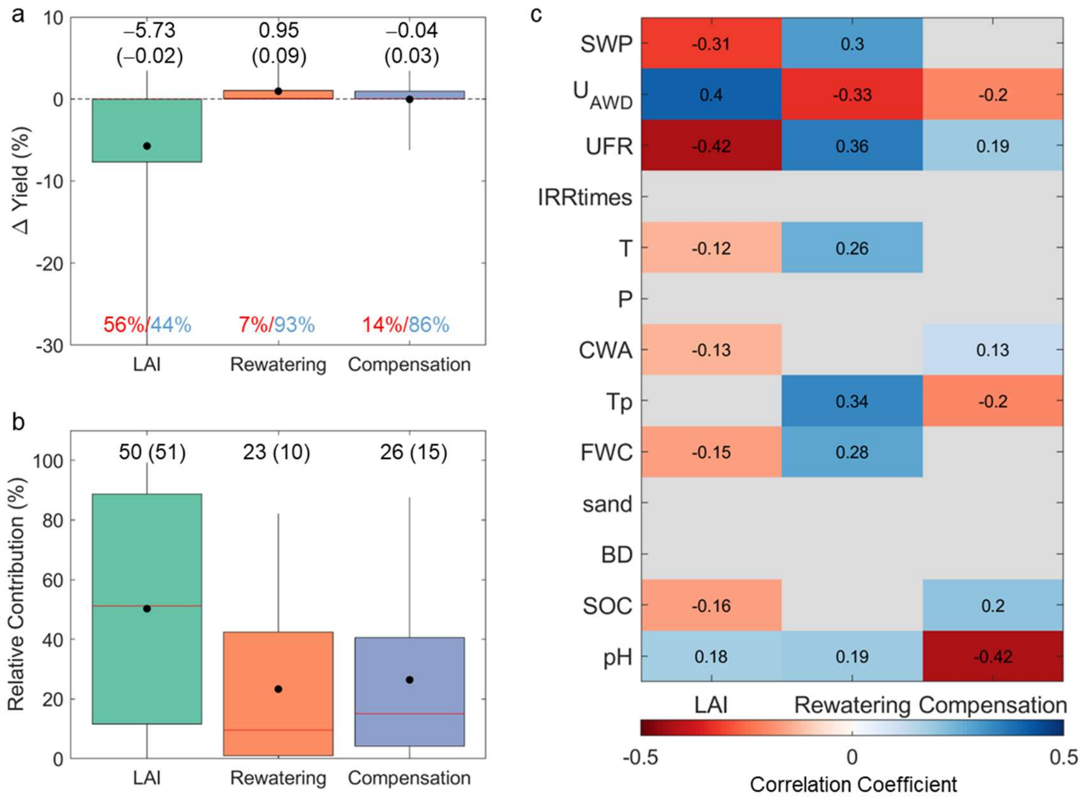

Figure S8 Contribution of physiological processes to ΔYield and relationship with predictors. (a) ΔYield induced by changes in leaf area expansion, rewatering effects and compensation effects. Numbers above the box indicate median (mean) values of ΔYield (%). Numbers below the box indicate proportion of total records with negative(red)/positive (blue) physiological effects. **(b)** Relative contributions of changes in leaf area expansion, rewatering effects and compensation effects to ΔYield. **(c)** Correlation coefficients between Relative contributions and environmental and management-related factors. *SWP*: Lower irrigation threshold indicated by soil water potential (kpa). U_{AWD}: Upper irrigation threshold (cm). *UFR*: Ratio of unflooded days to total growing days (%). *IRRtimes*: Irrigation times simulated by WHCNS. *T*: Mean daily growing season temperature (°C). *P*: Cumulative precipitation of growing season (mm). *CWA*: Cumulative precipitation minus potential evapotranspiration of growing season, representing water availability (mm). T_p: Potential transpiration (mm), indicating water requirements. *FWC*: Field water capacity (cm^3 cm^{-3}). *sand*: Soil sand content (%). *BD*: Soil bulk density (g cm^{-3}). *SOC*: Soil organic carbon (%). *pH*: soil pH.

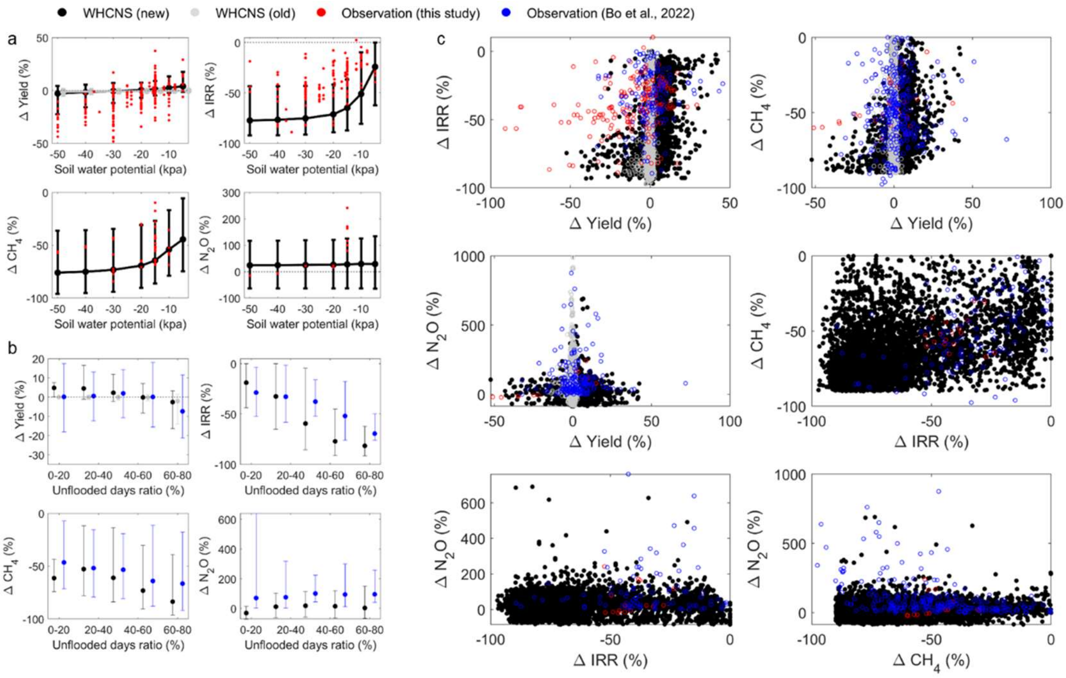

Figure S9 Scenario simulations and comparison with observations. **(a)** Comparison of changes in rice yield, irrigation water use, CH_4 and N_2O emissions (ΔYield, ΔIRR, ΔCH_4, ΔN_2O) in responses to soil water potential. **(b)** Comparison of ΔYield, ΔIRR, ΔCH_4, ΔN_2O in responses to unflooded days ratio. **(c)** Comparison of relationships between ΔYield, ΔIRR, ΔCH_4 and ΔN_2O. The dots indicate mean values and error bars show the 25-75th percentile range. The gray and black color indicate simulation results of the origin and modified WHCNS model, respectively. The red and blue color indicate observations compiled for this study and a previous study (Bo et al., 2022).

Reference

Bo, Y., Jägermeyr, J., Yin, Z., Jiang, Y., Xu, J., Liang, H., and Zhou, F.: Global benefits of non-continuous flooding to reduce greenhouse gases and irrigation water use without rice yield penalty, Global Change Biology, 28, 3636-3650, https://doi.org/10.1111/gcb.16132, 2022.

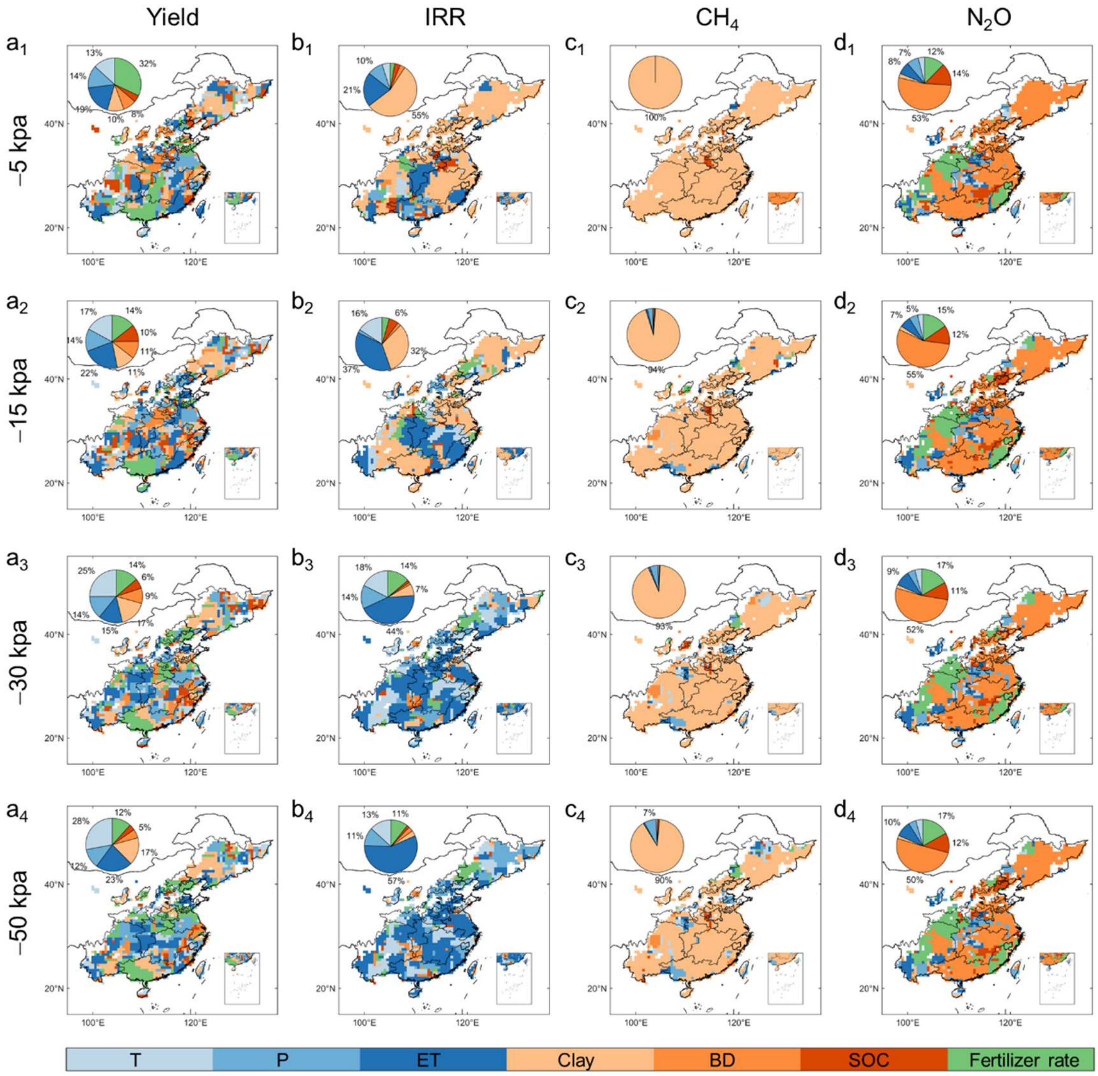

Figure S10 Distribution of dominant drivers regulating variation in relative changes of (a) Yield, (b) IRR, (c) CH_4, (d) N_2O. Each row represents results under lower irrigation threshold at −5, −15, −30 and −50 kpa. The inset pie plots represent the ratio (%) of irrigated rice areas for which relative changes variation is regulated by the dominant drivers. The dominant driver is defined as the factor with the largest absolute value of the correlation coefficient in each grid cell, identified from 3.5°-by-3.5° moving windows.

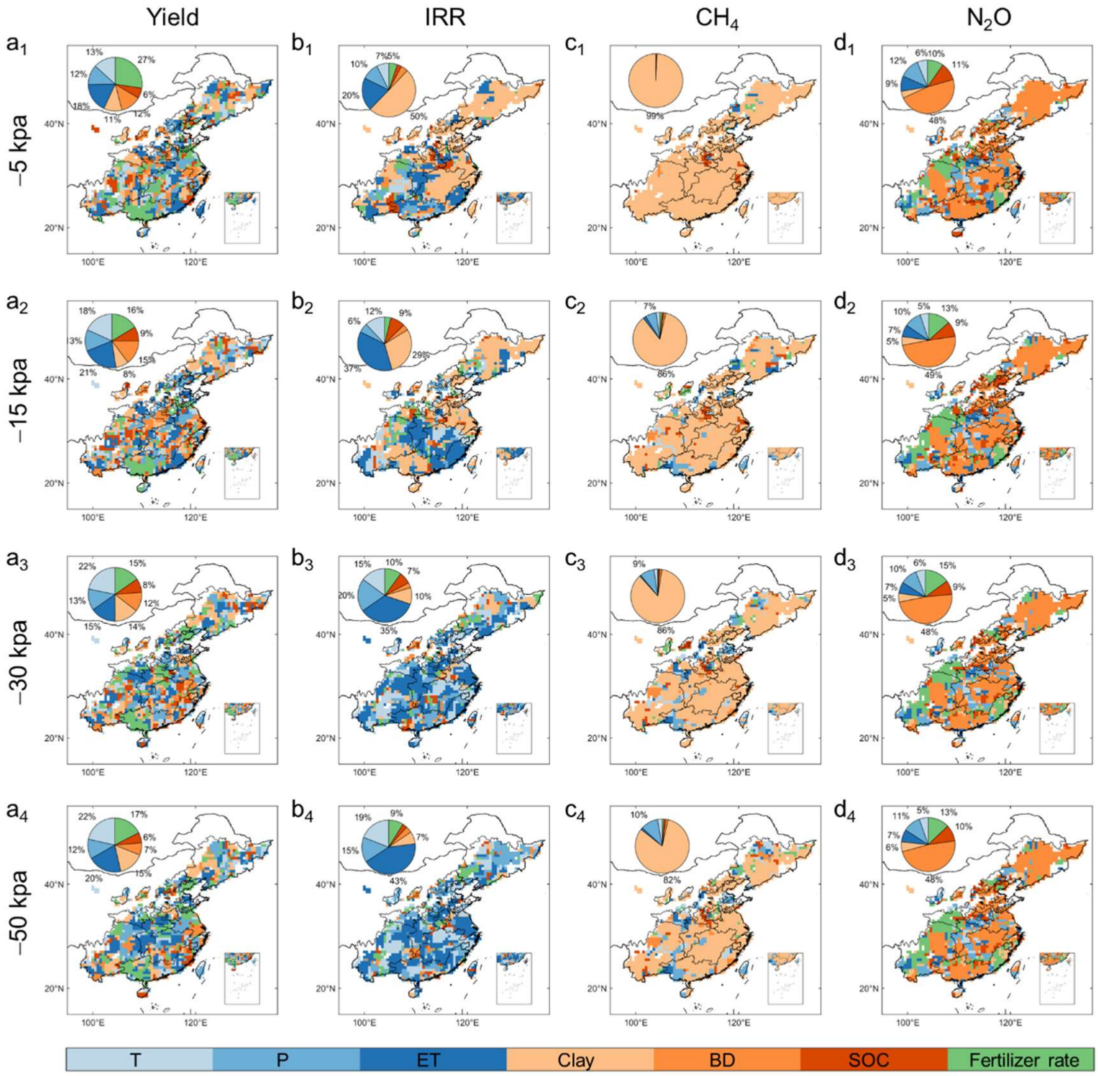

Figure S11 The same as Fig. S9 but for 2.5°-by-2.5° moving windows.

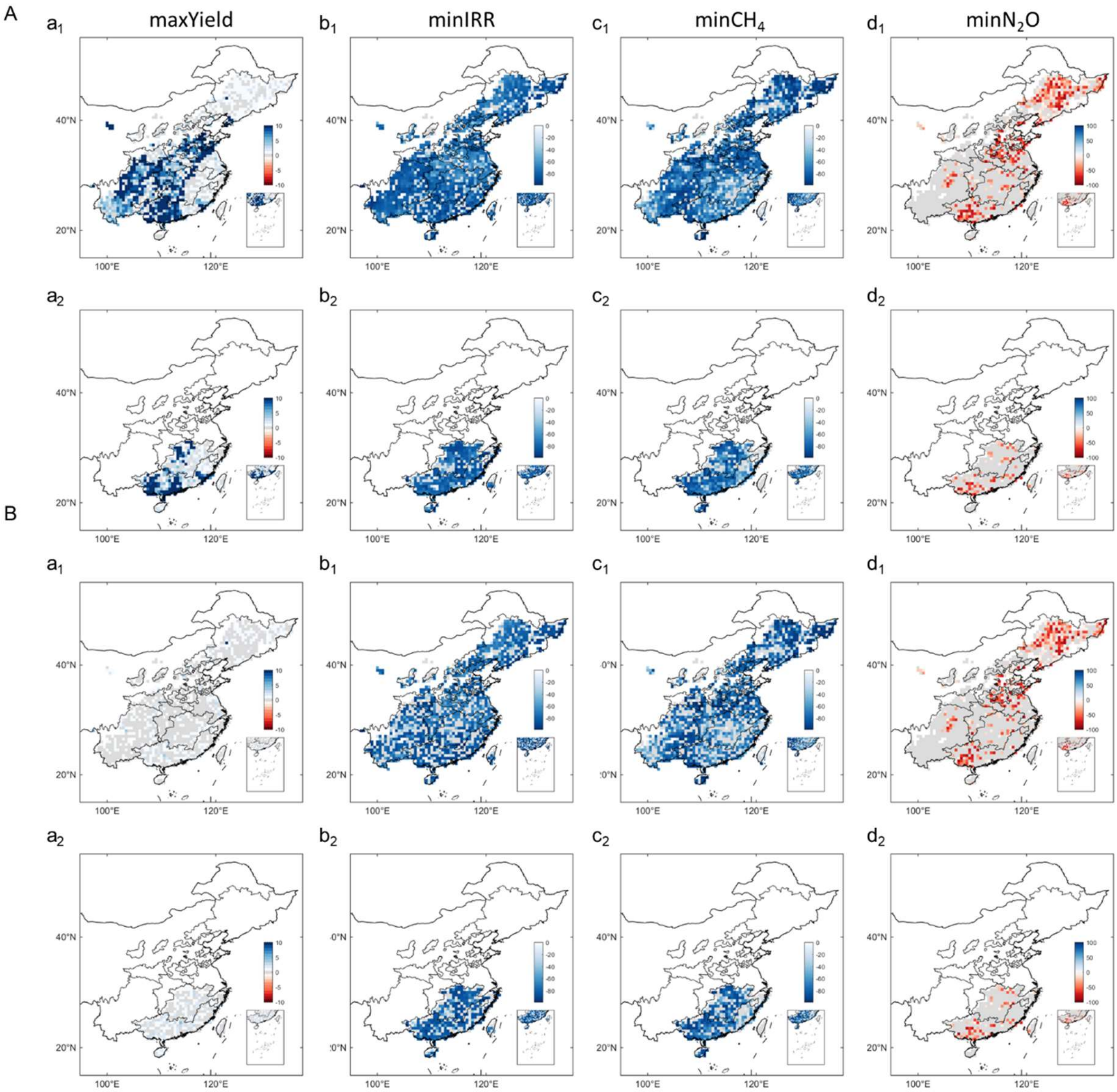

Figure S12 Spatial pattern of NCF benefits under four optimization targets based on the origin (A) and modified (B) model. The four columns correspond to four optimization targets, that are, maximized rice yield (*maxYield*), minimized irrigation water use (*minIRR*), minimized CH_4 emissions *minCH4*) and minimized N_2O emissions (*maxN2O*). The first and third rows show results for the major rice, and the second and fourth rows show results for the second rice growing season.

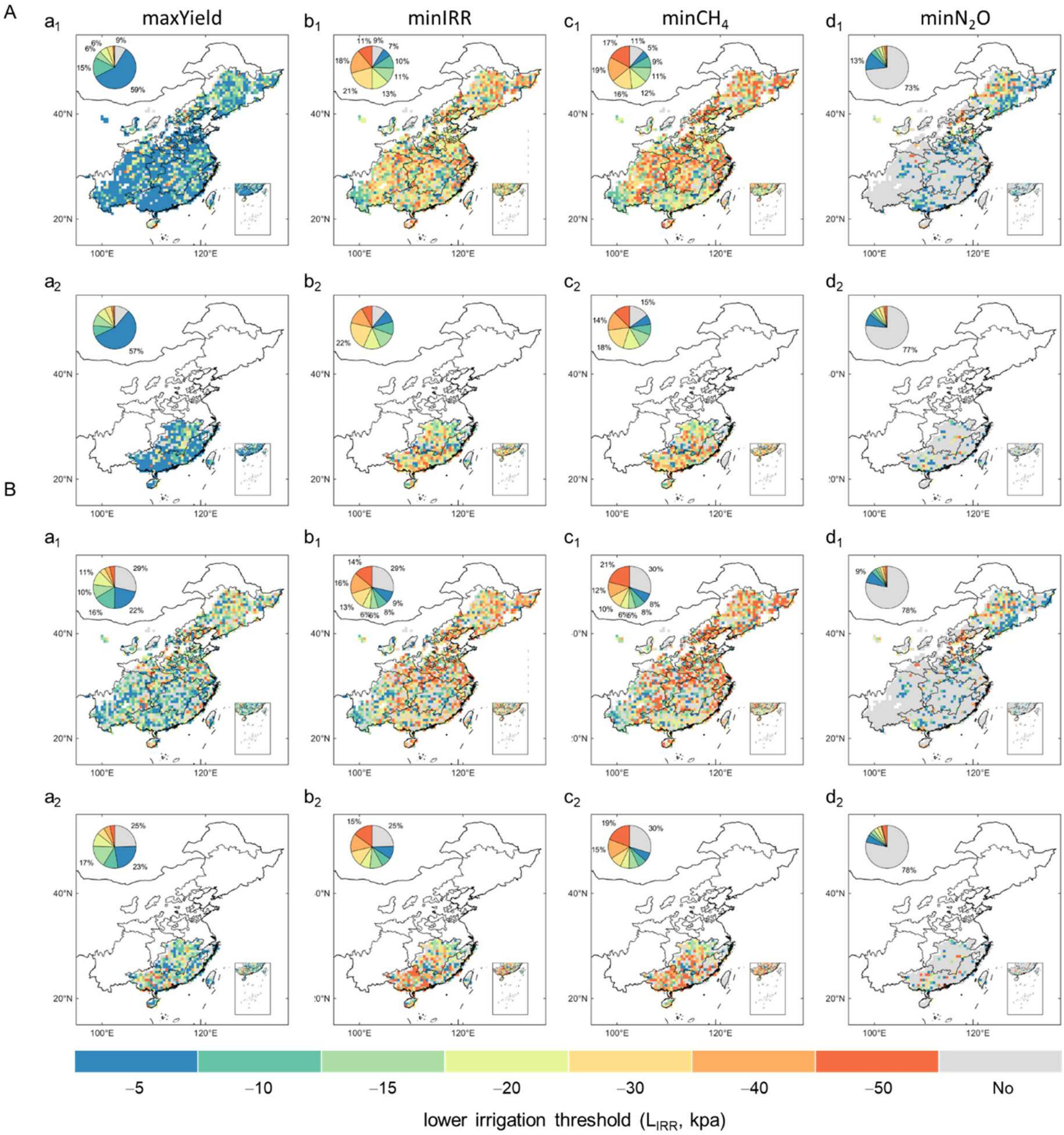

Figure S13 Spatial pattern of lower irrigation threshold under four optimization targets based on the origin (A) and modified (B) model. The four columns correspond to four optimization targets, that are, maximized rice yield (*maxYield*), minimized irrigation water use (*minIRR*), minimized CH_4 emissions *minCH₄*) and minimized N_2O emissions (*maxN₂O*). The first and third rows show results for the major rice, and the second and fourth rows show results for the second rice growing season. The inserted pies show proportions of rice areas with corresponding optimized lower irrigation thresholds (L_{IRR}) to total irrigated rice areas under the four single objective targets.

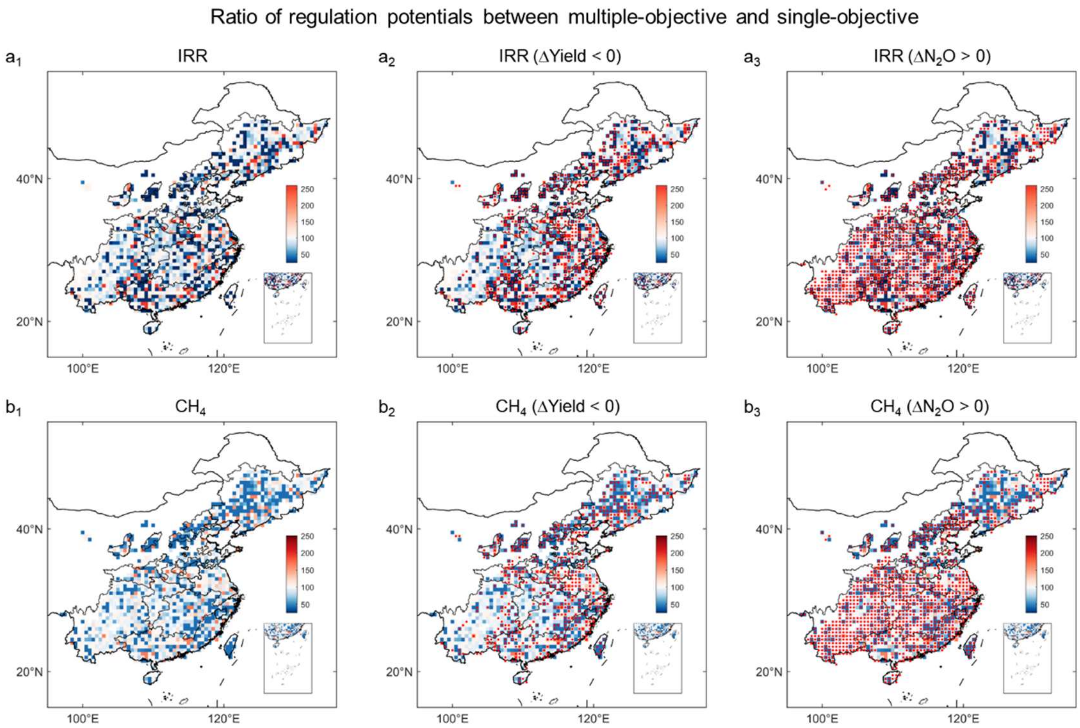

Figure S14 Tradeoffs between regulation potentials of different target variables. The plots show the ratio (%) of regulation potentials of IRR (a_1-a_3) and CH_4 (b_1-b_3) between multiple-objective and single-objective targets. The red dots indicate areas with decreased yield (a_2 and b_2) or increased N_2O emissions (a_3 and b_3) under multiple-objective target, highlighting regions with stronger tradeoffs between IRR (CH_4) reduction and yield increase or N_2O reduction.